The role pickup ions play in the termination shock

Daniel Ariad[1,*] and Michael Gedalin[1]

[1]*Department of Physics, Ben-Gurion University of the Negev, Beer-Sheva 8410501, Israel*

(Dated: 12 February 2013)

The termination shock (TS) is a quasi-perpendicular shock with broad regions on both sides that are populated by high energy ions. These energetic particles play an important role in the formation of the TS structure, which distinguishes it from planetary bow shocks. The pressure of the pickup ions is calculated by solving numerically the Vlasov equation in a time-stationary one-dimensional model shock with the parameters taken from the TS observations. The solution is obtained by backward tracing of the ion trajectories in the shock front. It is found that, in order to maintain the shock stationarity, the upstream density of the pickup ions should be comparable to the density of the solar wind (SW) protons.

I. INTRODUCTION

Recent observations of the termination shock [3, 5, 26, 31] have revealed that at this shock most of the energy of the incident ions is converted not into the downstream heated ion distribution but into high energy particles [5, 20] , which are (presumably) pick-up ions accelerated at the shock itself [7, 31]. It seems that it is these particles, instead these of the SW, that ensure maintenance of the shock profile by making possible Rankine-Hugoniot relations. Respectively, the energetic particles are, at least partially, responsible for the shock structure.

Measurements of the termination shock were made by Voyager 2 (V2) on 31 August - 1 September 2007 at a distance of 83.7 AU from the Sun. Data from the plasma and magnetic field instruments on V2 revealed that downstream the shock the heliosheath flow is not subsonic with respect to the thermal plasma. This indicated that non-thermal ion distributions probably have key roles in dynamical processes at the termination shock and in the heliosheath [26]. That lead to a speculation that unobserved energetic particles with energies that fall in the instruments energy gap contain the missing energy.

Heliosheath energetic neutral atoms (ENA) produced by charge exchange of suprathermal ions with interstellar neutral atoms were detected and mapped by STEREO A and B spacecraft (STE instrument), which orbits the sun at 1AU, from June to October 2007. Their energy spectra resemble those of solar wind pickup ions indicating that their parent ions are pickup ions energized by the termination shock. Their energy spectra imply that termination-shock-energized pickup ions with energies less then 0.028 MeV contain the missing energy dissipated in the termination shock, and they dominate the pressure in the heliosheath [31]. However, as pointed out by Hsieh et al. [14], the STE measurements of energetic electrons from the Sun could be affected by X-rays from Sco X-1, which brings substantial uncertainty into the conclusions of Wang et al. [31]. Extensive measurements of the line-of-sight integrated ENS fluxes by IBEX and by Cassini INCA [10, 17, 23] provided detailed all-sky images of ENAs in the low-energy range 0.1-10 KeV. In general, the measured fluxes are consistent with the expectation that the missing pressure required at the termination shock is provided by nonthermal ions (PUI). However, there is still substantial uncertainty of the estimates of PUI density in the termination shock vicinity. Nevertheless, Roelof et al. [27] combined the Voyager, Cassini INCA, and IBEX measurements within a generalized Rankine-Hugoniot analysis to estimate that "almost half of the downstream non-thermal pressure has to appear upstream of the termination shock".

Using a test particle approach, it was shown that for a sufficiently strong cross-shock potential and sufficiently narrow shock ramp, shock drift acceleration mechanism can produce particles with enough energy to account for the "missing" energy of the downstream SW plasma at the termination shock [4]. This has been shown for the perpendicular shock, while, according to the observations, the termination shock is substantially oblique [20]. Giacalone and Decker [12] incorporated pre-existing upstream magnetic turbulence within 2D hybrid simulations to study the combination of the acceleration at the ramp with the turbulent mechanism. The low energy end of the accelerated ions was reproduced but no high-energy tail was found, despite quite high turbulence level, probably because of the too coarse grid size which suppressed the acceleration at the ramp, sensitive to the ramp fine structure [36].

Recent observations of the structure of the termination shock [3] have shown that the energetic particle contribution to the overall pressure changes at the shock transition. In the same time, the solar wind pressure drops too much from upstream to downstream. Thus, the accelerated pickup ions should provide the missing part of the pressure to maintain the shock stationarity. These observations emphasize the necessity to comprehensively address the long-standing problem of the inter-relation of the shock structure and distribution of the accelerated particles [15, 18, 33]. Much effort has been invested so far into understanding of processes of pickup acceleration at quasi-perpendicular shocks [6–8, 19, 22, 35, 36], yet the research so far lacks the necessary synthesis of theory and observations. The influence of the high-energy distributions on the shock structure has not been consistently studied yet. This issue became acute with the discovery of the first shock where these energetic particles provide the main part of the ion pressure, and is extremely important for understanding of astrophysical shocks. In addition, understanding the interaction of the heliospheric shocks with high-energy populations

* daniel@ariad.org

is extremely important for understanding the propagation of energetic particles in the heliosphere [16]. In the present paper we use the backward numerical tracing of ion trajectories across the shock front to derive the pickup ion pressure and place the lower limit on the PUI upstream density required for the shock stationarity.

The paper is organised as follows. In Sec. 2 we present the model magnetic and electric profiles for the shock based on the observations. Sec. 3 describes the numerical method used to find the downstream velocity distribution. In Sec. 4 we analyse the solar wind protons crossing the shock. In Sec. 5 we numerically obtain the distribution of the accelerated PUI and derive their pressure. In Sec. 6 we discuss the role of the high energy tail. Discussion of limitations of the study and conclusions are given in Sec. 7.

II. THE SHOCK MAGNETIC AND ELECTRIC FIELDS

During the days 242-244 of year 2007 V2 crossed the TS at heliographic inertial (HGI) coordinates (83.66 AU, −27.5°, 216.3°) at least five times (only during three of them the telemetry was good enough). Due to the variations of the solar wind dynamics pressure or waves on the shock front, the termination shock moved back and forth [3, 26] at the time scale of a few hours (2-4 h), an order of magnitude longer than the gyroperiod, which is about 20 min in this case. In our analysis the shock crossing between 23:30 August 31 - 00:40 September 1, 2007 will be used. This crossing has the best data coverage to fit a magnetic field profile.

We adopt the shock normal (0.99,0.17,0.03) and upstream SW velocity (321.01,11.26,1.07) m/s as found by [20] using the velocity-magnetic field coplanarity method suggested by [1] combined with a Monte-Cralo method. The upstream SW velocity projection along the shock normal is 99.1% of its magnitude. That means that the shock measurements were done essentially in the normal incidence frame. Figure 1 shows the measured shock magnetic field in the shock coordinate system, where x is along the shock normal and $x-z$ is the coplanarity plane, as well as the fit used in the analysis.

The shock resembles a typical profile of a one dimensional, quasi-perpendicular shock with a classical structure consisting of a foot, ramp, and overshoot. Variations of B_x across the shock indicate that the shock structure may be not exactly one-dimensional and/or there are waves superimposed on the stationary profile. One has also to take into account that typically there are substantial errors in the determination of the shock normal direction. With only single spacecraft measurements it is difficult to estimate to what extent the shock is not one-dimensional and/or stationary. We shall stick to the above model approximation, shown in Figure 1, which is based on the widely accepted description of the supercritical shock [28].

In what follows we use the normalized quantities:

$$\mathbf{u} \equiv \frac{\mathbf{v}}{U_u}, \quad \mathbf{b} \equiv \frac{\mathbf{B}}{B_u},$$
$$\tau \equiv \Omega_u t, \quad \Omega_u = \frac{eB_u}{m_i},$$
$$e_y = \frac{E_y}{U_u B_u} = \sin\theta.$$

where $U_u = 320$ km/s is the upstream flow velocity, $B_u = 0.05$ nT is the upstream magnetic field, $E_u = B_u \cdot U_u$ is the upstream motional electric field, m_i is the proton mass, e is the proton charge, $\Omega_u = e \cdot B_u/m_i$ is the upstream proton gyrofrequency, and $\theta = 70°$ is the angle between the shock normal and the upstream magnetic field.

In our numerical analysis we use the following model shock profile proposed by Zilbersher and Gedalin [36], adapted for the observed termination shock:

$$b_x(x) = \cos\theta, \quad b_y(x) = 0, \tag{1}$$

$$\begin{aligned} b_z(x) = \sin\theta \Bigg[& 1 + \left(\frac{R_f - 1}{2}\right)\left(1 + \tanh 3\frac{x + D_f - 3D_r}{D_f}\right) \\ & + \frac{R_r - R_f}{2}\left(1 + \tanh\frac{3x}{D_r}\right) \\ & + (R_o - R_r)\exp\left(-2\frac{(x - D_o)^2}{D_o^2}\right) \\ & + \frac{R_d - R_r}{2}\left(1 + \tanh 3\frac{x - D_o - D_d}{D_d}\right)\Bigg] \end{aligned} \tag{2}$$

Here the coordinate is measured in the upstream ion convective gyroradii U_u/Ω_u, M is the Alfvenic Mach number, and θ is the angle between the shock normal and the upstream magnetic field. The parameters are chosen to reasonably fit the observed magnetic profile of the termination shock. The spatial scales of the termination shock were determined by taking the foot width approximately equal to $D_f = 0.4$ proton convective gyroradii [11]. Other length parameters scale according to the observed ratios of the lengths (crossing times) in the shock front [3]. Since the fit is done with a differentiable function, the positions of the shock structure elements can be determined only approximately. Indexed vertical lines in Figure 1 show the approximate positions of the beginning of the foot (a), beginning of the ramp (b), overshoot (c), beginning of the shoulder (d) and beginning of the downstream region (e), as given by applying (2).

For the electric field profile we adopt the widely accepted approximation [11, 21, 34]

$$e_x = -\alpha\frac{\partial b_z}{\partial x}, \quad e_y(x) = u_x b_z = \text{const}, \quad e_z(x) = 0 \tag{3}$$

Thus, the cross shock potential (CSP) is proportional to the variation of the main magnetic field component [see,e.g., 4]

$$\Phi = \alpha(b_z - \sin\theta), \quad e_x = -\frac{\partial\Phi}{\partial x} \tag{4}$$

This relation is a simplified extrapolation of the cold electron approximation, $E_x = -(B_z/4\pi ne)(dB_z/dx)$, for nearly perpendicular shocks with $n/B_z \approx$ const [cf. 36]. The nonzero

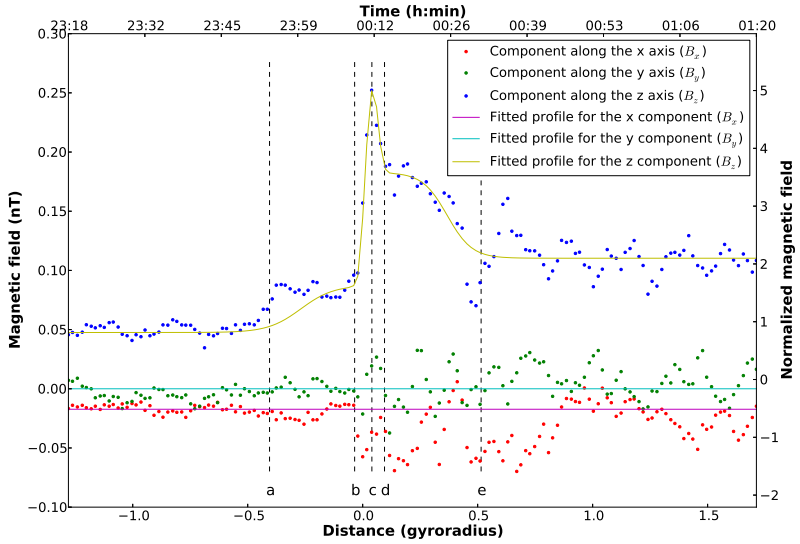

FIG. 1. Observed and fitted magnetic field profiles for the TS corresponding to the third crossing of the termination shock by V2 spacecraft magnetometer. The measured three components of the field, averaged over 48 sec segments and rotated into the standard shock related coordinates, with the superimposed fit given by (2) are plotted against time (upper horizontal axis) and coordinate along the shock normal (bottom horizontal axis, normalized with the upstream ion convective gyro radius). Indexed vertical lines show approximate locations of the beginning of the foot (a), beginning of the ramp (b), overshoot (c), beginning of the shoulder (d) and the beginning of the downstream region (e). Observations by Triaxial Fluxgate Magnetometer Experiment, Supported by NASA'a Voyager Interstellar Project (public domain). See also Burlaga et al. [3]. The data was obtained from NASA's National Space Science Data Center, Space Physics Data Facility.

electron temperature is approximately taken into account in the parameter α. The latter is determined by the requirement that the downstream distribution moments (flow speed, temperature and density), calculated numerically by a method based on Liouville mapping and which is described in the next section, will reasonably fit the V2 observations. The value of α, found in this way, makes the overall cross-shock potential, from far upstream to far downstream, equal to 0.17 of the upstream flow kinetic energy. The overall (upstream to downstream) cross-shock potential is significantly lower than the potential at the ramp, since the potential follows the magnetic field profile and the magnetic field decreases substantially behind the overshoot. However, it is the potential jump at the ramp that plays the major role in changing the ion velocity. The reason lies in the fact that the ramp is narrow enough to make the ion deflection due to the magnetic field negligible while the deceleration due to the electric field is significant. The cross-ramp potential here constitutes 0.45 of the upstream flow kinetic energy.

III. NUMERICAL METHOD

In this section we introduce a new method that evaluates numerically the downstream ions velocity distribution of the TS given the upstream distribution function. In what follows we assume that the shock can be considered as one-dimensional and stationary, that is, the electric and magnetic fields depend only on the coordinate along the shock normal and do not depend on time. These approximations are justified by the observations that the typical time scale of the shock reformation is much larger than the proton gyration period while the shock curvature radius is much larger than the gyroradius of the energetic ions. Let x be the coordinate along the shock normal. The collisionless Vlasov equation implies $f(t,\mathbf{r},\mathbf{v}) = \text{const}$ along the particle trajectory $\dot{\mathbf{r}} = \mathbf{v}$, $\dot{\mathbf{v}} = (e/m)(\mathbf{E} + \mathbf{v}\times\mathbf{B})$. In the one-dimensional stationary case one has, respectively, $f(x,\mathbf{v}) = f_0(x_0,\mathbf{v}_0)$, where it is implied that $x_0,\mathbf{v}_0$ and $x,\mathbf{v}$ belong to the same trajectory. Thus, one can build the ion distribution at the shock cross-section at x by tracing all possible trajectories back to the initial point x_0 where the distribution is known. It is worth noting that an ion can cross the same cross-section more than once (this is what actually happens since ions gyrate in the magnetic field) and the coordinates y and z along the shock front are ignored. This does not pose any problem since all these crossings correspond to the same value of the distribution function. The ion trajectory should be followed numerically until far upstream where the ion distribution is assumed known.

The equations of motion of the particles in average fields are time-reversible (if we replace t by $-t$, they will have the same form). For dissipation at a shock, we must have an irreversible process since entropy must increase. There is an additional process of scattering that ensures the irreversibility, which is caused by waves and turbulence. However, the effect of ion instabilities is negligible in the considered time scale.

In view of all above, the proposed mode of operation is as follows. The phase space at some x downstream is divided by a three dimensional grid into sufficiently small cells. The velocity in the center of each cell, $\mathbf{v}$, is assigned to an ion, which is further traced backward in time until the trajectory reaches some place x_0 sufficiently far upstream, where the

distribution is known. Then the cell is assigned the value of the distribution function corresponding to the velocity $\mathbf{v}_0$ which the ion has in the point x_0. If the ion trajectory does not reach upstream this cell is considered empty. To solve the ion equations of motion in the shock we use Runge-Kutta scheme of 4th order for velocity dependent forces [30].

IV. SOLAR WIND UPON CROSSING THE SHOCK

The objective of the analysis is to study the contribution of the solar wind protons and PUI into the overall pressure which is supposed to remain constant throughout a stationary one-dimensional shock. We start with the analysis of the solar wind crossing the shock. The upstream velocity distribution function, in accordance with observations [25], is taken in the form of the convected isotropic Maxwellian:

$$f(\mathbf{V}) = n_0(\pi\frac{2}{3}V_t^2)^{-3/2}\exp\left[-\frac{(\mathbf{V}-\mathbf{V_0})^2}{\frac{2}{3}V_t^2}\right] \quad (5)$$

where $n_0 = 1.3\times10^3$ m^{-3}, $V_t = 8.3$ km/s, and $\mathbf{V_0} = (320, 0, 0)$ km/s, respectively. The ion density and SW velocity are based on the mean values calculated by Li et al. [20] using velocity-magnetic field coplanarity. In the numerical analysis this SW distribution was taken at $x_0 = -1.7$ ion convective gyroradii ahead of the shock foot. Figure 2 shows the number density of protons per velocity magnitude, defined as follows:

$$F(x,v) = \int f(x,\boldsymbol{v})v^2\sin\theta d\theta d\varphi \quad (6)$$

where $\boldsymbol{v} = v(\sin\theta\cos\varphi, v\sin\theta\sin\varphi, \cos\theta)$. The value of $F(x,v)$ is shown by color. The obtained moments of the distribution function across the shock are plotted in Figure 3. The hydrodynamic velocity and pressure tensor components are spatially periodic behind the ramp because of the gyration of the downstream distribution as a whole and slow gyrophase mixing [cf. 24]. These oscillations are clearly seen in high-resolution measurements at the termination shock (see Fig. 3 by Richardson et al. [26]).

The pressure tensor is anisotropic, $\Pi_{zz} \ll \Pi_{xx} \sim \Pi_{yy}$. Momentum conservation across a stationary one-dimensional shock can be written as follows:

$$M_k \equiv [\Pi_{xk} + \frac{B^2}{2\mu_0}\delta_{xk} - \frac{B_xB_k}{\mu_0}] = \text{const} \quad (7)$$

Theis is a vectorial relation, of which the most important is the x component which states the pressure balance throughout the shock. If the M_x varies substantially with x that means that the shock is not stationary and/or not one-dimensional. It is convenient to represent the pressure balance in the following dimensionless form:

$$\frac{v_x}{v_u} + \frac{\Pi_{PUI,xx}}{n_um_iV_u^2} + \frac{1}{2M^2}\left(\frac{B}{B_u}\right)^2 + \frac{\beta_i}{2M^2}\left(\frac{p_i}{p_{iu}}\right) + \frac{\beta_e}{2M^2}\left(\frac{p_e}{p_{eu}}\right) = \text{const} \quad (8)$$

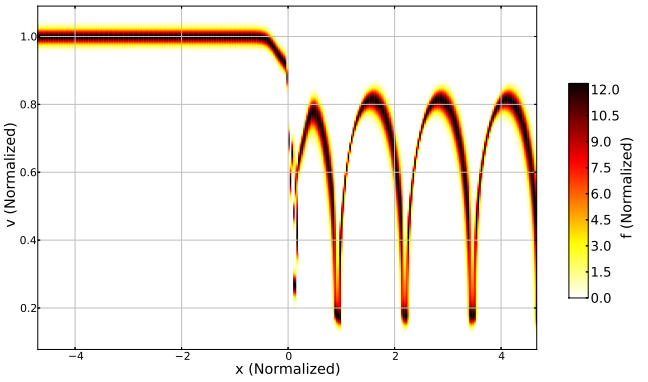

FIG. 2. The phase space density $F(x,v)$ for solar wind protons. The coordinate x is normalized with the upstream proton convective gyroradius U_u/Ω_u, the velocity v is normalized with the solar wind velocity U_u, and F is normalized with n_u/U_u, where n_u is the upstream density of the solar wind.

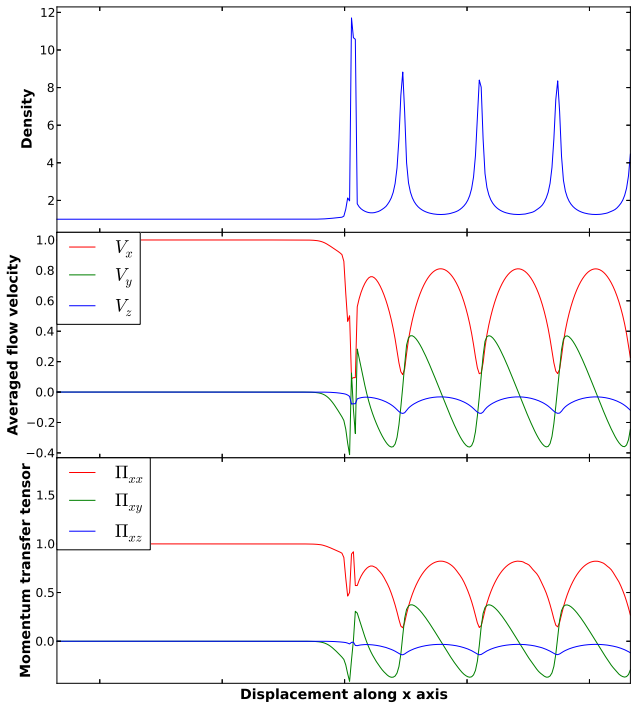

FIG. 3. Top to bottom: the number density, the mean velocity along the shock normal, and the relevant pressure tensor components for the solar wind across the shock, normalized with the corresponding upstream values.

For the termination chock parameters [20, 26], $M \approx 8$, nearly cold upstream plasma, $\beta \ll 1$, modest compression, $v_u/v_d = n_d/n_u \approx B_d/B_u \approx 2$, and weak heating, $T_{id}/T_{iu} \approx 10$, $T_{ed}/T_{id} \sim 0.1$, nearly 40% of the pressure would be missing downstream unless PUI contribution. At the overshoot, the magnetic pressure constitutes about 20% of the upstream dynamic pressure of the solar wind, so that the missing pressure should be provided by PUI throughout. Even with electrons taken into account the deficiency of the down-

stream pressure is too large to satisfy the RH conditions. Thus, SW alone cannot support the shock. This result is backed by the observations which imply that ions with energies outside the range of PLS observation spectrum, $10 - 5950eV$, contribute significantly to the total pressure. It is believed that the population of energetic particles in the range of $6 - 10keV$, which gain energy via acceleration and the shock front, may contribute the missing pressure [4, 31, 35, 36]. It is worth noting that PUI contribute to the upstream pressure also.

V. ACCELERATED PICKUP ION DISTRIBUTION AND PRESSURE

The observed heating of the solar wind protons amounts up to 4% of the energy lost by the ions crossing the shock [25, 26]. This indicates that the incident SW kinetic energy had to be transferred to some other particle population, possibly accelerated PUIs. The shock drift acceleration is known as an energization mechanism of PUI [2, 32]. PUI were shown to be accelerated in TS to high energies by multiple reflection [4, 19, 22, 35, 36]. We analyze the distribution of PUI in the same way as we did for solar wind protons.

Since the actual PUI distribution in the TS upstream is not known precisely, a simplified form of PUI distribution, filled-shell centred at SW flow velocity, is used. It was derived theoretically [29] and verified by SWICS and HISCALE observations near heliospheric shocks by observing He^{+} and He^{++} ions [13].

$$f_{upstream}(v) = A_0(1 - H(v-u))\left(\frac{v}{u}\right)^{-1.5}\exp\left(-\left(\frac{v}{u}\right)^{-1.5}\right). \quad (9)$$

Here v and u are the particle velocity and the SW upstream flow speed, respectively, while $H(v)$ is the step function. The coefficient A_0 is unknown and will be determined from the requirement that the RH relations should be satisfied. The corresponding density function $F(x,v)$ for accelerated PUI throughout the shock front is plotted in Figure 4. The SDA mechanism spreads the downstream velocities range to ~125% of the spread in the upstream, and breaks the distribution symmetry.

Total M_x together with the solar wind and PUI contributions are plotted in Figure 5. The coefficient $A_0 = 2.2 \cdot 10^{-15}$ $m^{-3}/(m/s)$ is chosen so to ensure that the mean downstream M_x be equal to the mean upstream M_x.

It is seen that in order that the PUI contribution be sufficient to support the shock stationarity, their upstream density should be rather high, about 0.4 of the SW upstream density. This result was not entirely unexpected. Wang et al(2008) observed heliosheath ENA. These ENA are remote traces of energetic ion populations in distant regions, as they retain the parent ion's velocity in the change exchange process. It was shown that, if the ENA parent heliosheath ions come from the energization of the population by the TS, their spectrum should extend down to the SW energies. It was therefore concluded that their density must be comparable to that of the SW [31]. (See, however, Hsieh et al. [14] for possible complications in the interpretation of the measurements.)

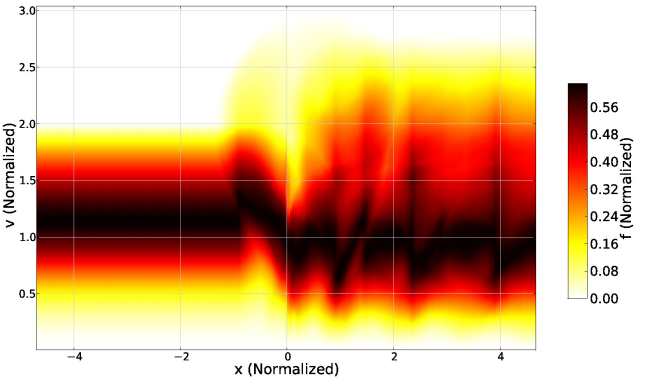

FIG. 4. The number density $F(x,v)$ for PUI. Normalization as in Figure 2.

VI. HIGH ENERGY TAIL

In the analysis above we concentrated on the low-energy end of the accelerated PUI spectrum. Yet, the observed spectrum is much wider. The V2 is equipped with an LECP instrument that measures ions density per energy in an energy spectrum of $0.028 - 3.5$ MeV using eight energy-bands. Daily averages of the ion density per velocity in V2's eight channels are shown in Figure 6. The daily averages are well fitted with a power law of the form $f(v) = A(v/u_{SW})^{\alpha}$, where u_{SW} is the upstream SW flow velocity, α is the spectral index, and A is constant. No significant variations in the immediate vicinity of the shock were observed in those energy channels while V2 crossed the TS. The average spectral index and amplitude at the shock are $\alpha = -2.4 \pm 0.1$ and $A = 5.9 \times 10^{-6} \pm 2.8 \times 10^{7}$ $m^{-3}(m/s)^{-1}$, respectively [5].

The total number density of PUI at the shock, in the energy range of $0.028 - 3.5$ MeV, is 0.1 m^{-3} which is %0.01 of SW upstream density. Assuming isotropic pressure, the diagonal elements in the upstream region can be estimated as ~%1 of the total SW pressure. Thus, this high energy tail does not contribute noticeably to the total pressure in the shock vicinity, and, therefore, should not be taken into account in Rankine-Hugoniot relations. This tail was not found in the above numerical analysis because of the somewhat simplified model of the shock front. Indeed, observations [3] show that the shock transition itself is substantially structured (see Fig. 7, top panel). It has been shown [36] that such fine structure makes the acceleration more efficient so that PUIs are accelerated to higher energies. In order to study the effect of the fine structure here we added "teeth" with a similar width and height as observed to the shock ramp profile. This was done modulating the magnetic field given by(2) with the function $\sum_{n=0}^{4}\sin\left(b\left(x+c_n\right)\right)/\left(x+c_n\right)$, where $b = 6 \cdot 10^{-11}/B_u$, and $c_n = \frac{4-2n}{10}D_r$ (see Fig. 7, bottom panel). The model potential is taken as earlier, see (4).

The same numerical analysis has been performed for the structured shock. Figure 8 shows the PUI energy distributions, $N(E) = f(v)(dv/dE) \propto f(\sqrt{(E)})\sqrt{E}$ found numerically for the smooth (top) and structured (bottom) shocks, at the distance

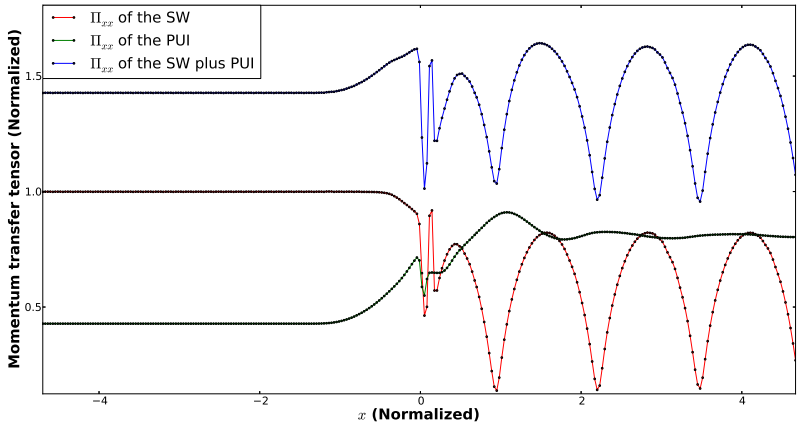

FIG. 5. Total M_x (blue), solar wind pressure (red) and PUI pressure (black).

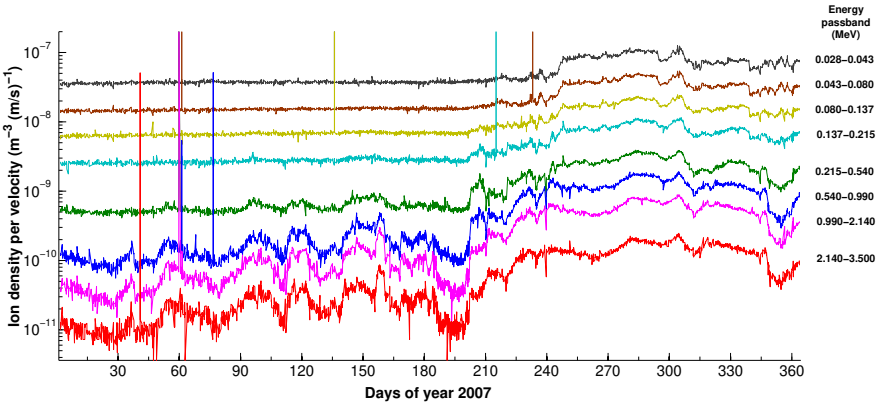

FIG. 6. Daily averages of the ion density per velocity in eight Voyager 2 ion channels using good sectors average (1,2,3,5,6,7) calculated with proton energy passbands and efficiencies. Observations by Low Energy Charged Particle Instrument, Supported by NASA'a Voyager Interstellar Project (public domain). See also Decker et al. [5]. The data was obtained from NASA's National Space Science Data Center, Space Physics Data Facility.

of 15 upstream convective gyroradii downstream of the shock.

The high energy tail goes up to higher energies for the structured shock. It is easily seen that the low-energy body distribution is nearly flat. The contribution to the pressure is $P \propto \int N(E)EdE$. For the low energy core roughly $N(E) \propto E^{-\alpha}$, $\alpha < 1$, and the highest energies determine the pressure. The flat distribution lasts up to several solar wind proton energies, beyond which it sharply drops by about an order of magnitude until the spectrum can again be approximated with a power-law $N(E) \propto E^{-\alpha}$, $\alpha > 2$. The contribution of this high energy tail to the pressure is, therefore, determined by $N(E)$ at the lowest energy of the tail, and is negligible relative to the contribution of the low-energy body core. Thus, while the high energy rail is expected to affect the gradual mediation of the shock at scales much larger than the ion gyroradius, it does not show up in the Rakine-Hugoniot relations at the shock itself.

Adding the fine structure to the ramp in our numerical analysis increased the maximum energy that PUI gains by an order of magnitude, at most. The maximum energy we obtained here was about 10 times the SW proton energy (i.e. about 5 keV) while the measured highest energies were up to 7000 times higher (i.e about 3.5 MeV). The acceleration efficiency is sensitive to the angle between the shock normal and the upstream magnetic field, to the scale of the ramp substructure, and to the cross-shock potential [4, 19, 22, 35, 36]. If the shock is rippled the local shock normal can be substantially different from the global normal found from coplanarity. The shock may be more close to the perpendicular geometry locally, which may result in higher energies of the accelerated ions and harder distribution tail. There may be also errors in the determination of the shock scale and the cross-shock potential may be underestimated.

According to the observations, the intensity of energetic particles rose exponentially during the 40 days (about 10^3 ion convective gyroradii) that preceded the V2 encounter with the TS and reached a plateau 7 days after V2 crossed the TS. In addition the SW flow velocity decreased from 380 km/s far upstream to about 300 km/s at the shock. Florinski et al. [9] showed that that the gradual slowdown of the SW during last 40 days of V2 observations in the SW is plausibly explained by the pressure energetic particles exert on the back-ground plasma,

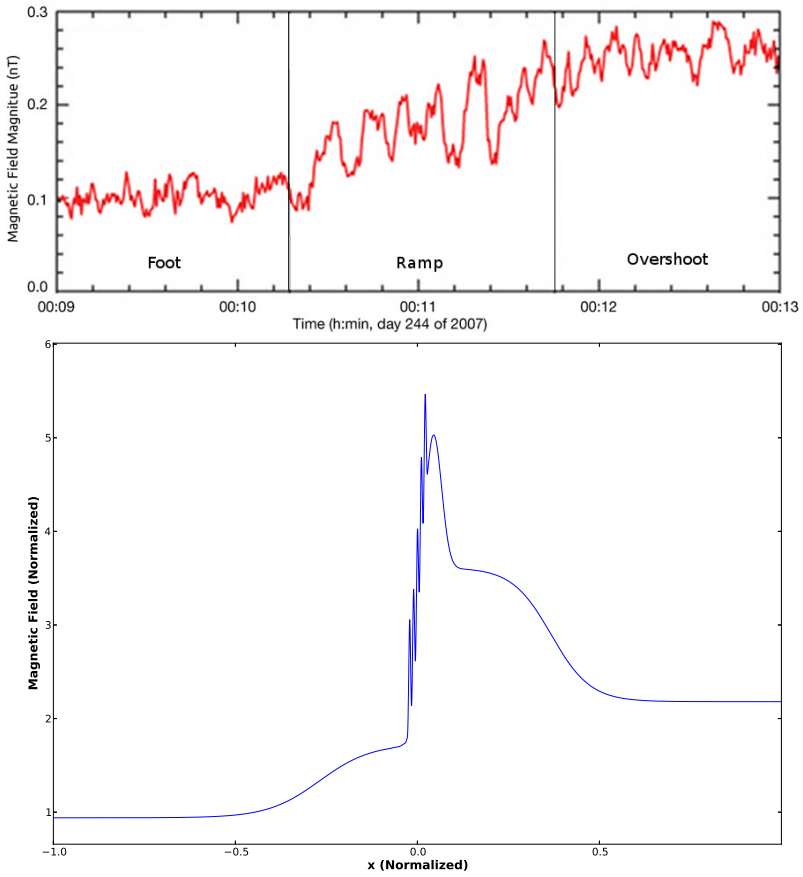

FIG. 7. Top: Magnetic field magnitude measured by Voyager 2 Triaxial Fluxgate Magnetometer (MAG) at 0.48 sec intervals. The MAG the vector magnetic field at rate of 2.08 samples per second [3]. Only the ramp is shown. Bottom: model approximation of the measured magnetic field.

based on gas-dynamic conservation laws. They assumed the shock was stationary and that the diffusion coefficient did not vary along the shock normal. This study shows that first order Fermi acceleration might be the mechanism that is responsible for this energetic population.

VII. CONCLUSIONS AND DISCUSSION

We have studied the pickup ion dynamics within the termination shock and their contribution to Rankine-Hugoniot relations - pressure balance or momentum conservation across the shock front. In our analysis we used a model approximation for the magnetic field measured by V2 at the shock crossings when the observations seemed to be of best quality. In contrast with the previous work regarding the shock as perpendicular [4], we analyzed an oblique geometry with the shock angle $\theta_{Bn} = 70^{\circ}$, in accordance with the shock parameters deduced from observations [20]. For the analysis the cross-shock potential was adjusted so that the downstream ion velocity and temperature resemble the observed values. The derived downstream temperature in our calculations is several times higher than the observed ones, which may indicate that the cross-shock potential was somewhat underestimated. Yet, we preferred to leave it as it is, instead of trying a better fit, since in this case we obtain the lower limit on the PUI density required to maintain pressure balance across the shock. The study has been done by following ion trajectories back in time followed by Liuoville mapping to the upstream distribution which is assumed to be known.

Taking into consideration only the SW protons populations, which has approximately Maxwellian distribution, in our numerical calculation kept essence of the momentum conservation problem. The computation showed that almost 40% of the pressure was missing, in close agreement with the observations [26].

We have found that pickup ions, distributed as a filled shell just upstream of the shock, undergo efficient surfing/multiple reflection energization. The far downstream distribution grows a substantial super-thermal energy tail up to 10 times of the solar wind proton energy (depending on the fine structure of the ramp). The downstream distribution consists of a rather flat low-energy body and a high-energy power-law tail. It is the low-energy body which contributes the missing pressure, while the contribution of the high energy tail at the shock transition is negligible. In order to ensure pressure balance the upstream density of PUI should be comparable to the solar wind density. We find that the lower limit of the density ratio is

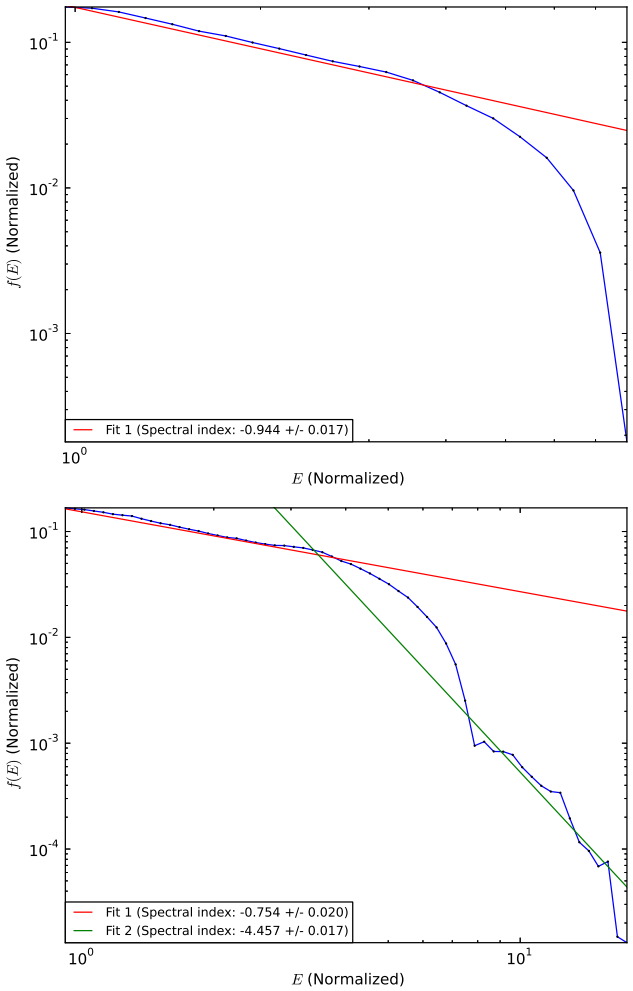

FIG. 8. Energy distribution (relative units) for smooth ramp (top) and serrated ramp (bottom). Energy is normalized on the energy of the solar wind proton.

$\approx 40\%$. Earlier observations of ENA by STEREO A and B [31] provided the estimates of the PUI density of $\sim 1.6 \times 10^3 m^{-3}$ which is about 75% of the SW. Thus, Liouville mapping with the test particle analysis of a model shock provides a rather good agreement with observations. The one-dimensional stationary model use here does not take into account possible shock rippling or time-dependence. Yet, the basic physics is reproduced sufficiently well.

Observations by V2 shown a high energy power law spectrum (0.028 – 3.5 MeV). The intensity of the most energetic ions started to increase about 770 gyroradii before the TS. This was accompanied with a decrement of the SW flow speed from about 380 km/s to about 300 km/s, which began far upstream and ended at the TS. This observation could not be explained by our deterministic test particle approach which accelerated particles only up to 3.9keV, nor the SW speed decrement which began only about 1.7 gyroradius before the shock. Florinski et al. [9] found from observations that the average diffusion coefficient for energetic particles (1 – 3.5 MeV) was $10^{16}(m^2\ s^{-1})$. They showed that the precursor of the quantities mentioned above can be explained by First order Fermi acceleration [9]. The length scale of the slowdown is the diffusive length (D/U, where D is the momentum-averaged value of the radial diffusion coefficient and U is the flow speed). The radial diffusion length scale is about 470 gyroradii, which entails that the diffusion effects are irrelevant for SDA.

[1] B. Abraham-Shrauner, Determination of magnetohydrodynamic shock normals, J. Geophys. Res.*77,* 736, 1972.

[2] T. P. Armstrong, M. E. Pesses, and R. B. Decker, Shock drift acceleration, *Washington DC American Geophysical Union Geophysical Monograph Series*, 35, 271, 1985.

[3] L. F. Burlaga, N. F. Ness, M. H. Acuña, R. P. Lepping, J. E. P. Connerney, and J. D. Richardson, Magnetic fields at the solar wind termination shock, *Nature, 454,* 75, 2008.

[4] R. H. Burrows, G. P. Zank, G. M. Webb, L. F. Burlaga, and N. F. Ness, Pickup Ion Dynamics at the Heliospheric Termination Shock Observed by Voyager 2, *Astrophys. J., 715,* 1109, 2010.

[5] R. B. Decker, S. M. Krimigis, E. C. Roelof, M. E. Hill, T. P. Armstrong, G. Gloeckler, D. C. Hamilton, and L. J. Lanzerotti, Mediation of the solar wind termination shock by non-thermal ions, *Nature*, 454, 67, 2008.

[6] L. A. Fisk, G. Gloeckler, and T. H. Zurbuchen, Acceleration of Low-Energy Ions at the Termination Shock of the Solar Wind, *Astrophys. J., 644,* 631, 2006.

[7] V. Florinski, Pickup Ion Acceleration at the Termination Shock and in the Heliosheath, *Space Sci. Rev., 143,* 111, 2009.

[8] V. Florinski, R. B. Decker, and J. A. le Roux, Pitch angle distributions of energetic particles near the heliospheric termination shock, *J. Geophys. Res., 113,* 7103, 2008.

[9] V. Florinski, R. B. Decker, J. A. le Roux, and G. P. Zank, An energetic-particle-mediated termination shock observed by Voyager 2, *J. Geophys. Res., 36,* 12101, 2009.

[10] H. O.Funsten, F. Allegrini, G. B. Crew, R.DeMajistre, P. C.Frisch, S. A.Fuselier, M.Gruntman, P.Janzen, D. J.McComas, E.Möbius, B.Randol, D. B.Reisenfeld, E. C.Roelof, N. A.Schwadron, Structures and Spectral Variations of the Outer Heliosphere in IBEX Energetic Neutral Atom Maps, *Science, 964,* 326, 2009.

[11] M. Gedalin, Ion reflection at the shock front revisited, *J. Geophys. Res., 101,* 4871, 1996.

[12] J. Giacalone and R. Decker, The Origin of Low-energy Anomalous Cosmic Rays at the Solar-wind Termination Shock, ApJ*, 91,* 710, 2010.

[13] G. Gloeckler, L. A. Fisk, and L. J. Lanzerotti, Pickup Ions Upstream and Downstream of Shocks, In G. Li, G. P. Zank, & C. T. Russell, editor, *The Physics of Collisionless Shocks: 4th Annual IGPP International Astrophysics Conference*, volume 781 of *American Institute of Physics Conference Series*, pages 252–260, August 2005.

[14] K. C. Hsieh, P. C.Frisch, J. Giacalone, J. R Jokipii, J. Kóta, D. E. Larson, R. P. Lin, J. G. Luhmann and L.Wang, A Re-Interpretation of STEREO/STE Observations and Its Consequences, *Astrophys. J. Lett., 79,* 694, 2009.

[15] J. R. Jokipii, J. Giacalone, and J. Kóta, The physics of particle acceleration at the heliospheric termination shock, *Planet. Space Sci., 55,* 2267, 2007.

[16] M. B. Kallenrode, Acceleration and propagation of energetic charged particles in the inner heliosphere, *Nucl. Phys. B Proc. Suppl., 39,* 45, 1995.

[17] S. M.Krimigis, D. G.Mitchell, E. C.Roelof, K. C.Hsieh and D. J.McComas, Imaging the Interaction of the Heliosphere with the Interstellar Medium from Saturn with Cassini, *Science, 971,* 326, 2009.

[18] M. A. Lee and L. A. Fisk, Shock acceleration of energetic particles in the heliosphere, *Space Sci. Rev., 32,* 205, 1982.

[19] M. A. Lee, V. D. Shapiro, and R. Z. Sagdeev, Pickup ion energization by shock surfing, *J. Geophys. Res., 101,* 4777, 1996.

[20] H. Li, C. Wang, and J. D. Richardson, Properties of the termination shock observed by Voyager 2, Geophys. Res. Lett.*35,* 19107, 2008.

[21] P. C. Liewer, V. K. Decyk, J. M. Dawson, and B. Lembege, Numerical studies of electron dynamics in oblique quasi-perpendicular collisionless shock waves, J. Geophys. Res.*96,* 9455, 1991.

[22] A. S. Lipatov, G. P. Zank, and H. L. Pauls, The acceleration of pickup ions at shock waves: Test particle-mesh simulations, J. Geophys. Res.*103,* 29679, 1998.

[23] D. J. McComas, H. O. Funsten, S. A. Fuselier, W. S. Lewis, E. Mobius, and N. A. Schwadron, IBEX observations of heliospheric energetic neutral atoms: Current understanding and future directions, Geophys. Res. Lett.*38,* L18101, 2011.

[24] Ofman, L., M. Balikhin, C.T. Russell, and M. Gedalin, Collisionless relaxation of ion distributions downstream of laminar quasi-perpendicular shocks, J. Geophys. Res.*114,* A09106, 2009.

[25] J. D. Richardson, Plasma temperature distributions in the heliosheath, Geophys. Res. Lett.*35,* 23104, 2008.

[26] J. D. Richardson, J. C. Kasper, C. Wang, J. W. Belcher, and A. J. Lazarus, Cool heliosheath plasma and deceleration of the upstream solar wind at the termination shock, *Nature, 454,* 63, 2008.

[27] E. C.Roelof, S. M.Krimigis, D. G.Mitchell, R. B.Decker,J. D.Richardson, M.Gruntman and H. O.Funsten, Implications of Generalized Rankine-Hugoniot Conditions for the PUI Population at the Voyager 2 Termination Shock, *American Institute of Physics Conference Series*, 133-141–1302,2010.

[28] J. D. Scudder, T. L. Aggson, A. Mangeney, C. Lacombe, and C. C. Harvey, The resolved layer of a collisionless, high beta, supercritical, quasi-perpendicular shock wave. I - Rankine-Hugoniot geometry, currents, and stationarity, J. Geophys. Res.*91,* 11019, 1986.

[29] V. M. Vasyliunas and G. L. Siscoe, On the flux and the energy spectrum of interstellar ions in the solar system, J. Geophys. Res.*81,* 1247, 1976.

[30] F. Vesely, *Computational Physics: An Introduction*, Kluwer Academic/Plenum Publishers, 2001.

[31] L. Wang, R. P. Lin, D. E. Larson, and J. G. Luhmann, Domination of heliosheath pressure by shock-accelerated pickup ions from observations of neutral atoms, *Nature, 454,* 81, 2008.

[32] G. M. Webb, W. I. Axford, and T. Terasawa, On the drift mechanism for energetic charged particles at shocks, ApJ*270,* 537, 1983.

[33] K.-P. Wenzel, Charged particle acceleration processes in the interplanetary medium, *Adv. Space Res., 9,* 179, 1989.

[34] J. R. Wygant, M. Bensadoun, and F. S. Mozer, Electric field measurements at subcritical, oblique bow shock crossings, J. Geophys. Res.*92,* 11109, 1987.

[35] G. P. Zank, H. L. Pauls, I. H. Cairns, and G. M. Webb, Interstellar pickup ions and quasi-perpendicular shocks: Implications for the termination shock and interplanetary shocks, J. Geophys. Res.*101,* 457, 1996.

[36] D. Zilbersher and M. Gedalin, Pickup ion dynamics at the structured quasi-perpendicular shock, *Planet. Space Sci., 45,* 693, 1997.